

Two-wave method of laser-stimulated oxidation of the porous silicon layer

© L.V. Grigoryev^{1,2}, A.A. Semenov², A.V. Mikhailov³

¹ St. Petersburg State University,
199034 St. Petersburg, Russia

² St. Petersburg State Electrotechnical University „LETI“,
197022 St. Petersburg, Russia

³ JSC Vavilov State Optical Institute“,
199101 St. Petersburg, Russia

e-mail: lvgrigoryev@mail.ru

Received August 20, 2023

Revised August 20, 2023

Accepted December 27, 2023

A new method of photon-stimulated surface treatment of a semiconductor is described the method of two-spectral laser-stimulated oxidation of a layer of porous silicon. The results of studying the optical properties of a layer of laser-oxidized nanoporous silicon in a spectral band are presented. The initial layer of nanoporous silicon was obtained by electrolytic etching of the surface of the single-crystal silicon KDB-10 (100) according to generally accepted method. The density of anode etching was 25.0 mA/cm². A laser-stimulated oxidation of a nanoporous silicon layer was carried out using two laser radiation lengths of unequal intensity at a fundamental wavelength of 1.064 μm using a DPSS YAG: Nd laser operating in a pulsed mode. The laser wavelengths for the photon-stimulated assay mode was 980 nm, 520 nm, and 405 nm.

Keywords: Photon-stimulated surface treatment, laser-stimulated oxidation, laser-oxidized nanoporous silicon, X-ray diffraction, transmission spectra, structure integral optics.

DOI: 10.61011/EOS.2023.12.58183.5501-23

Introduction

The rapid development of integrated optics, radio photonics, and, especially, silicon photonics in recent decades allows us to expect the creation of specialized optical processors based on them for real-time signal processing in the near future. Therefore, there is a need for new methods of forming integrated-optical structures for radio photonics and integrated optics devices operating in the spectral range up to 1.6 μm based on silicon or containing silicon [1–6] nanoclusters in their volume. The use of such silicon structures containing silicon nanoclusters will make it possible to fabricate planar waveguides with nonlinear optical properties, integrated-optical switches, emitters for silicon optocouplers, integrated-optical cavities, and microphotonic sensors that can be incorporated into microphotonics and integrated optics devices [1–5,7–10]. In this connection, it is necessary to carry out research focused on the creation of new electron-ionic methods of surface treatment (such as laser, ion-plasma, and electron-beam methods) for semiconductors and dielectrics [7–10]. Laser technology benefits from reproducibility, process cycle controllability, vacuum purity, and the ability to be incorporated into the existing planar microelectronics and microphotonics [1,10] process technology. The present study is a continuation of research into the possibility of production (in particular, by laser-stimulated methods) of integrated-optical structures based on oxidized porous silicon [11–15]. Unlike previously published papers, this study describes a new method of

photon-stimulated modification of the surface of porous silicon and formation of silicon nanocomposites without the use of an aggressive oxidant gas medium in the technological process and without unique laser equipment (HF laser). The process of photon-stimulated semiconductor surface treatment by accompanying laser radiation was designed to alter the optical parameters of this semiconductor due to the generation of non-equilibrium charge carriers in the near-surface region of the treated semiconductor.

This paper presents the results of examination of changes in the optical properties of a layer of porous silicon subjected to photon-stimulated oxidation. A nanoporous silicon layer was simultaneously exposed to radiation from two lasers with different wavelengths. Auxiliary radiation was provided by three different laser diodes with wavelengths of 980, 520, and 405 nm, while primary radiation was the one of a YAG:Nd DPSS laser operating in pulsed mode with a wavelength of 1.064 μm.

Experimental setup for photon-stimulated surface treatment

The initial layer of nanoporous silicon was created by electrochemical etching of the surface of single-crystalline silicon in a horizontal fluoroplastic Uno–Imai reactor. The regime of electrolytic etching is similar to that described in [7–9]. A layer of porous silicon with pore sizes ranging from 5 to 15 nm [7,8] was produced in this regime.

Further oxidation of the nanoporous silicon layer was carried out using a modified laser setup with two laser channels: a laser diode for photon-assisted treatment of the surface (three different laser diodes operated at 980, 520, and 405 nm) and the primary technological pulsed laser operating at a wavelength of $1.064\ \mu\text{m}$. The machine was equipped with an optical scheme for combining two laser beams into one working field and a system of two-axis scanning by the beam of the process laser. The primary process laser was based on a DPSS YAG:Nd laser ($1.064\ \mu\text{m}$) operating in pulsed-periodic mode. Irradiation of the surface of the porous silicon layer was carried out by repeatedly scanning the beam over the area with the pulse energy of the process laser falling within the 0.35–0.4 mJ range and the pulse duration being 20–23 ns. When used to move the micromirror in the scanner, a piezo actuator could not establish the needed linear mode of beam scanning over the working area, since this piezo actuator had hysteresis. Therefore, an electromagnetic actuator was used to move the micromirror in the scanner. The scanned laser beam had a Gaussian energy distribution in the cross section. The laser beam radius was $250\ \mu\text{m}$ in the surface processing plane. The following laser diodes were used for photon-assisted treatment: D6-4-980-50-N (wavelength — 980 nm, power — 50 mW), D6-6-520-50 (wavelength — 520 nm, power — 50 mW), and JLD405NM20MW (wavelength — 405 nm, power — 20 mW). Radiation was collimated by a quartz condenser onto the treated surface through a free-hanging mask with an opening $5 \times 5\ \text{mm}$ in size. Oxidation was carried out under normal conditions in an air atmosphere.

Structural studies of a laser-modified porous silicon layer

It was found by microscopy that there were no regions of explosive vaporization and silicon melt spatter in the oxidation zone. Thus, in contrast to the results previously published in [11–15], in the present work it was possible to optimize the technological mode of laser-stimulated oxidation of a layer of porous silicon by using an assisting source of laser radiation in the technological channel of the unit with photon energies comparable to the width of the bandgap of single-crystal silicon.

We used the X-ray diffraction method to investigate the morphology of laser-oxidized nanoporous silicon layers, which allowed us to identify all polymorphic modifications of SiO_x silicon oxides and estimate the degree of structural perfection of silicon dioxide obtained as a result of laser-stimulated treatment of the porous silicon layer. X-ray diffraction studies were carried out using a DRON-7 automated X-ray diffractometer. The range of scanning angles 2θ was from 10 to 40° . A copper anode with a filter was the source of CuK_α X-ray radiation.

For radiographic studies of SiO_x , four ranges of angles 2θ are of the utmost interest: from 18 to 25° , from 26 to 27° ,

from 31 to 33° , and from 34 to 37° . It is in these angle ranges that all the basic information (type of diffraction profile, its half-width, and angular position), which allows us to evaluate the structural properties of silicon dioxide obtained as a result of laser treatment, is concentrated.

The difference between structural forms of silicon dioxide is determined by its crystal chemistry and synthesis conditions [10,16–18]. Each silicon atom has a quaternary position, i.e., is tetrahedrally surrounded by four oxygen atoms, each of which is bridging. Through a common oxygen atom, SiO_4 tetrahedrons bond to each other at different angles to form a continuous three-dimensional lattice. The values of Si–O–Si angles and Si–O distances vary in rather wide ranges, which naturally affects the strength of oxygen–silicon bonds. The mutual arrangement of SiO_4 tetrahedrons in space specifies one or another modification of silicon dioxide. The domain of stable existence of each phase of silicon dioxide is determined by the temperature conditions of its synthesis. Phase transitions are accompanied by the breaking and transformation of bonds. At a temperature of 573°C , trigonal α -quartz transforms into hexagonal β -quartz with a slightly expanded crystal lattice. Further heating of silicon oxide leads to its transformation into cubic α - SiO_2 (high-temperature cristobalite) and to an almost threefold increase in the lattice cell volume of SiO_2 . In practice, this allows to use such a phase transition to remove isomorphic impurities and possible gas and liquid inclusions from quartz in the process of formation of thin films. The most structurally advanced form is trigonal α - SiO_2 . In addition to trigonal α - SiO_2 , such polymorphic modifications of β - SiO_2 as tridymite and cristobalite are characterized by a high degree of structural perfection.

It should be noted that high-temperature modifications of silica with higher symmetry of the crystal structure (β -quartz, β -cristobalite, and β -tridymite) are considered unstable [15–18]. Thus, they transform necessarily into α -forms of silicon dioxide upon cooling. At high temperatures, re-layering proceeds along the (111) crystallographic direction in the ideal structure of cubic α - SiO_2 . As the temperature decreases, the number of layers increases; the strict spatial three-dimensional ordering is also broken, which is reflected in the diffraction pattern as broadening of the corresponding diffraction line.

Depending on the laser exposure conditions, the porous silicon layer subjected to laser-stimulated oxidation is transformed into silicon dioxide containing both high-temperature trigonal modification α - SiO_2 and various α - SiO_2 phases of the cristobalite type and polymorphic β - SiO_2 modifications.

For sample No. 1 (Fig. 1), sequential heating of a porous silicon layer by a laser beam with a wavelength of $1.064\ \mu\text{m}$ and UV stimulation of the heating zone leads to heating of the treatment zone under the laser beam to temperatures of 1350°C . This is evidenced by the observed phase transition and a diffraction pattern containing reflections corresponding to different modifications of quartz (peaks A–E). Figure 1 shows that in addition to the

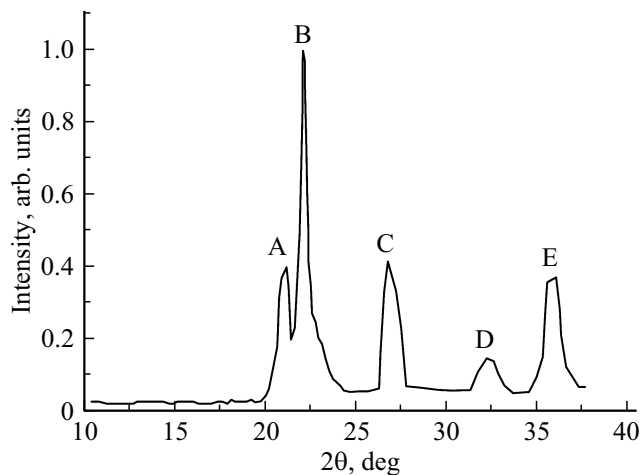


Figure 1. Diffraction pattern of sample № 1.

diffraction reflections belonging to α quartz (peaks A, B, C), reflections belonging to other β phases (peaks D and E) appeared in the diffraction pattern. With the help of a reference database, we have determined that heating a layer of porous silicon to 1350°C resulted in the formation of two other modifications in addition to α -quartz: β -cristobalite and α -tridymite (hexagonal, tetragonal, and orthorhombic lattices, respectively). In addition, due to cooling of the working zone after laser treatment, partial crystallization of the sample occurred and two phases (tetragonal β -cristobalite and orthorhombic α -tridymite) were formed.

For sample No. 2 (Fig. 2), the porous silicon layer was heated by a laser beam with a wavelength of 1.064 μm and the heating zone was illuminated by accompanying radiation with a wavelength of 520 nm. This led to the generation of non-equilibrium charge carriers in the near-surface area, changing significantly the reflection and transmission coefficients of the semiconductor material under the laser spot. All these factors suggest the following: under the beams of two lasers, the treatment zone is heated to a temperature of 1350°C. This is evidenced by the observed phase transition and a diffraction pattern containing reflections corresponding to different modifications of quartz (peaks A, B, C, D). Figure 2 shows that in addition to the diffraction reflections belonging to α quartz (peaks A, B and C), reflections belonging to other β phases (peak D) appeared in the diffraction pattern. In comparison with Fig. 1, it should be noted that in Fig. 2 there is no peak in the diffraction pattern corresponding to β -phases of silicon oxide and located around an angle of 32°. Laser heating of the porous silicon layer with two wavelengths, 1.064 μm and 532 nm, results in a temperature of 1350°C at which α -quartz phases are synthesized and another modification (β -cristobalite) is formed.

For sample No. 3 (Fig. 3), the porous silicon layer is heated by two wavelengths: a laser beam with a wavelength of 1.064 μm and IR radiation with a wavelength of 980 nm. In this case, the diffraction pattern undergoes

cardinal changes in comparison with those considered earlier. Specifically, only three peaks A, B, and C are present in the diffraction pattern. Previously considered in Figs. 1 and 2, two nearby peaks A and B corresponding to the α -quartz reflections and located at an angle around 23°, are transformed, according to Fig. 3, into single peak A, which has a bell-shaped appearance. No reflections corresponding to one of the β -cristobalite phases are also seen in the diffraction pattern (Fig. 3). It should be noted that the peaks (reflections) are narrower than their counterparts in Figs. 1 and 2. It should be emphasized that photon-stimulated laser beam exposure with accompanying illumination of the working area with IR radiation was carried out at the primary wavelength of 1.064 μm and neither duration nor energy in the laser pulse was changed. In this context, it may be assumed that the near-surface area of the porous silicon layer is heated to temperatures exceeding 1350°C. Therefore, it can be stated that laser-stimulated oxidation of the porous silicon layer produces forms of α -quartz and one β -quartz modification (cristobalite). After the laser beam leaves the zone of exposure, the modified (i.e., oxidized to various forms of quartz) layer cools in accordance with the same thermophysical laws that were shown earlier. This also leads to the formation of phases of tetragonal β -cristobalite and orthorhombic α -tridymite.

Study of the optical properties of an oxidized porous silicon layer

Figure 4 shows the spectral dependence of the transmission coefficient of the investigated samples in the 2.0–17.0 μm band. All measurements of the investigated samples were carried out using a BRUKER VERTEX 70 IR Fourier spectrometer on a layer of nanoporous silicon separated from the substrate and a layer of laser-oxidized porous silicon separated from the substrate. The transmittance of the original porous silicon layer in this spectral band was no higher than 55%. As can be seen from Fig. 4,

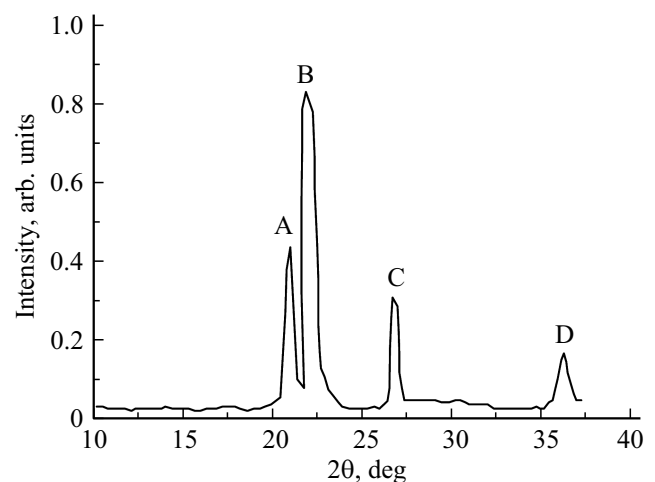


Figure 2. Diffraction pattern of sample № 2.

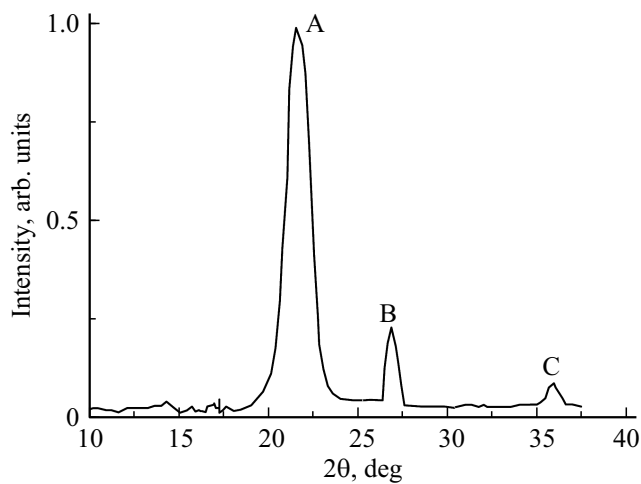


Figure 3. Diffraction pattern of sample № 3.

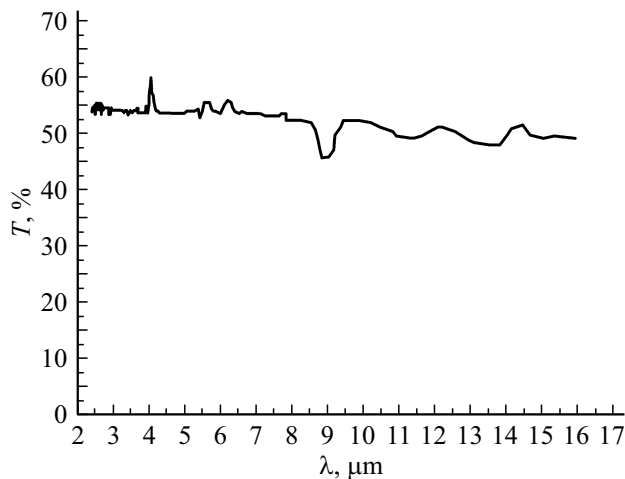


Figure 4. Spectral dependence of the transmission coefficient of the porous silicon layer.

the spectral dependence shows absorption regions due to the presence of water vapor and hydroxyl groups bound to silicon in silicon pores. Absorption bands corresponding to bending and valence vibrations of O–Si–O bridges are also present (bands 8–9.5, 10–12, and 12.5–14.5 μm), but their intensity is low.

Figure 5 shows the transmission spectra of the porous silicon layer subjected to laser oxidation with assisting photon illumination of the porous silicon surface at different wavelengths. For all three transmission spectra considered, the $T(\lambda)$ dependence takes the form of a complex monotonic curve with eight large local minima, which are located in the following spectral bands: 2.5–3.2 μm (region A), 3.3–3.44 μm (region B), 4.16–4.35 μm (region C), 5.55–6.25 μm (region D), 7.0–10.0 μm (region E), 11.0–12.2 μm (region F), and 12.5–13.3 μm (region G). The highest value of $T(\lambda)$ is 65%. Comparing the transmission spectra presented in Fig. 5 with the transmission spectrum of laser-oxidized nanoporous silicon

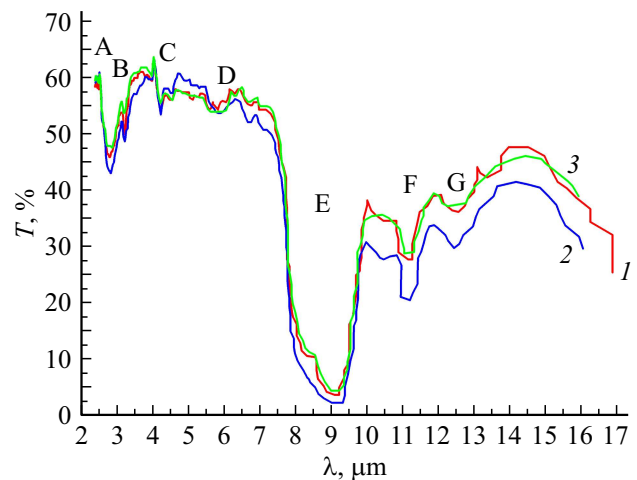


Figure 5. Spectral dependence of the transmission coefficient of laser-oxidized porous silicon: surface illumination by laser radiation with a wavelength of 520 (1), 402 (2), 980 nm (3).

from [14], one can see that the absorption in the 12.5–13.3 μm region is significantly weaker during laser oxidation without accompanying photon illumination. That said, the absorption in the 7.0–10.0 μm band is the strongest. In the case of photon-assisted laser-stimulated oxidation of the porous silicon layer, the $T(\lambda)$ plot is dominated by the 7.0–10.0 μm spectral band, where the transmittance of the laser-oxidized silicon layer decreases to 3%, while a transmittance of 38% was obtained in this spectral band in [14]. This 7.0–10.0 μm spectral band (region E) may be associated with bending and valence vibrations of Si–O bridges in the Si–O–Si system. An intense absorption band in this spectral range is typical of the Si–SiO₂ system with a developed Si–O–Si interface [7–9,12–15], which confirms that laser-stimulated oxidation of the porous silicon layer has occurred.

The next minimum observed in the transmission coefficient plot in the 11.5 μm region, according to [8,9,13,15], can also be attributed to bending and valence vibrations of Si–O bridges. The presence of this intense absorption band also confirms the oxidation of porous silicon and the formation of a developed Si–O–Si interface in the created silicon composite. In addition, in the transmission spectra of thermally oxidized porous silicon reported in [1–3], the highest absorption was also observed in the 7.5–11.0 μm band. This suggests a predominantly thermal mechanism of silicon dioxide phase formation during laser-stimulated photon-assisted oxidation of the porous silicon surface.

Thus, a significant absorption in the 7.5–10.5 μm spectral band in all three samples allows us to conclude that a dielectric matrix of silicon dioxide with inclusions of silicon nanoclusters in its volume formed in the process of laser-stimulated oxidation. At the same time, the lack of obvious minima of the transmission coefficient in the $T(\lambda)$ spectral dependence in the range of 14.5–16.6 μm allows us to state that the obtained layer of nanoporous silicon was practically

free of contamination from SiH_x-groups. In addition, the transmission spectra of samples subjected to laser oxidation with photon-assisted surface treatment showed a decrease in transmittance, which is typical of the formation of the borosilicate glass phase (a band with a minimum in transmittance at 7.14 μm). This spectral band corresponds to valence vibrations of the B–O system. In the spectral band around 10.2 μm corresponding to the B–O–Si bond, the $T(\lambda)$ value decreases from 65 to 35%. It should be said that the $T(\lambda)$ spectral dependence measured in [11–14] at laser oxidation without photon stimulation revealed no absorption bands typical of the formation of borosilicate glass in the volume of the silicon nanocomposite layer.

Thus, by spectral methods it was possible to find out that when the layer of nanoporous silicon is simultaneously exposed to laser radiation with a wavelength of 1.064 μm and accompanying radiation with wavelengths of 980, 520, and 405 nm, a layer of dielectric matrix of silicon dioxide containing borosilicate glass in its volume is formed. For the previously studied samples of oxidized porous silicon subjected to thermal or laser oxidation in a strong oxidant medium [12,15], the spectral dependences of the transmission coefficient lacked regions characteristic of the formation of the borosilicate glass phase.

Conclusion

The method of stimulating the semiconductor surface by laser radiation with wavelengths of 980, 520, and 405 nm made it possible to oxidize the porous silicon layer by laser radiation with a wavelength of 1.064 μm without destroying the treated surface. The $T(\lambda)$ spectral dependence of oxidized porous silicon showed the presence of intense absorption bands corresponding to different phases of silicon oxide and silicon dioxide formed in the composite.

In laser-oxidized porous silicon, no traces of contamination by SiH_x-groups were detected by the spectral method. In all three investigated samples of laser-oxidized porous silicon, it was possible to detect a formed borosilicate glass phase. The proposed technology of porous silicon surface modification by a two-wave method allows one to form layers of high-quality oxidized porous silicon, which can be used to create waveguide, nonlinear, or resonator integrated-optical structures compatible with the existing planar technology of microelectronics and microphotonics devices.

The method of laser-vector patterning of integrated-optical structures makes contact microlithography redundant, thus simplifying significantly and reducing the cost of production of devices for microphotonics and radio photonics.

Conflict of interest

The authors declare that they have no conflict of interest.

References

- [1] K. Djordjev, C. Seung-June, C. Sang-Jun, R.D. Dapkus. *IEEE Photonics Technol. Lett.*, **14**, 828-30 (2002).
- [2] G. Martinez-Jimenez, Y. Franz, A.F. Runge, M. Ceschia, N. Healy, S.Z. Oo, A. Arazona, H.M. Chong, A.C. Peacock, S. Mailis. *Opt. Mater. Express*, **9** (6), 2573, (2019). DOI: 10.1364/OME.9.002573.
- [3] Y. Franz, A.F.J. Runge, S.Z. Oo, G. Jimenez-Martinez, N. Healy, A. Khokhar, A. Tarazona, H.M.H. Chong, S. Mailis, A.C. Peacock. *Opt. Express*, **27** (4), 4462 (2019).
- [4] G.Z. Mashanovich, M.M. Milosevich, M. Nedeljkovic, N. Owens, B. Xiong, E.J. Teo, Y. Hu. *Opt. Express*, **19** (8), 7113 (2011).
- [5] X.J. Wang, T. Nakajima, H. Ishiki, T. Kimura. *Appl. Phys. Lett.*, **95**, 040906 (2009).
- [6] F.Y. Gardes, D.J. Thomson, N.G. Emerson, G.T. Reed. *Opt. Express*, **19** (12), 11804 (2011).
- [7] A.G. Gullis, L.T. Canham, P.D. Calcott. *J. Appl. Phys.*, **82** (3), 909 (1997).
- [8] O. Bisi, S. Ossieni, L. Pavesi. *Surf. Sci. Rep.*, **38**, 1 (2000).
- [9] L. Pavesi. *J. Phys.: Cond. Matt.*, **15**, 1169 (2003).
- [10] U. Das, V. Sadasivan. *J. Las. Opt. Photon.*, **4** (2), 1000163 (2017). DOI: 10.4172/2469-410X.1000163
- [11] L.M. Sorokin, V.I. Sokolov, A.P. Burtsev, A.E. Kalmykov, L.V. Grigor'ev. *Tech. Phys. Lett.*, **33** (12), 1065 (2007).
- [12] L.V. Grigor'ev, A.V. Mikhailov. *J. Opt. Technol.*, **81** (10), 616 (2014).
- [13] L.V. Grigor'ev, A.V. Mikhailov. *J. Opt. Technol.*, **82** (11), 777 (2015).
- [14] L.V. Grigor'ev, S.O. Solomin, D.S. Polyakov, V.P. Veiko, A.V. Mikhailov. *J. Opt. Technol.*, **83** (7), 429 (2016).
- [15] L.V. Grigor'ev, P.P. Konorov, A.V. Mikhailov. *J. Opt. Technol.*, **79** (2), 99 (2012).
- [16] T. Inokuma, Y. Wakayama, T. Muramoto, R. Aoki, Y. Kurata. *J. Appl. Phys.*, **83**, 2228 (1998). DOI: 10.1063/1.366951.
- [17] L.X. Yi, J. Heitmann, R. Scholz, M. Zacarias. *Appl. Phys. Lett.*, **81**, 4248 (2002). DOI: 10.1063/1.1525051
- [18] K. Sato, T. Izumi, M. Iwase, Y. Show, H. Morisaki, T. Yaguchi. *Appl. Surf. Sci.*, **216**, 376 (2003).

Translated by D.Safin